SHOCK WAVE REFLECTION IN GAS–LIQUID FOAMS

A. T. Malakhov and B. I. Palamarchuk

UDC 532.529+532.593

Shock wave propagation in gas–liquid foams was studied in [1-5]. It was established in [1, 2] that plane shock waves in foams have developed relaxation zones with pressure rise times up to several milliseconds. Then with increase in intensity the parameters of incident, and especially reflected, waves deviate from the equilibrium parameters in a foam, calculated in the manner of [6], from the volume concentration of the condensed phase (c-phase). To describe the process of shock wave reflection in gas–liquid systems [4] proposed a model approach based on description of shock compression of a two-phase medium by a polytropy index $K = 1 + (\gamma - 1)(1 - \varepsilon)$, where γ is the adiabatic index of the Poisson gas phase, and ε is the volume concentration of the c-phase. Despite this approach's satisfactory description of the experiments of [1, 2] on shock wave reflection in foam, use of K to explain observed shock wave attenuation in foam leads to severe divergence between experimental and calculated data [7, 8]. One of the causes of disagreement of calculated and experimental shock wave parameters in foam is apparently the presence of developed relaxation zones, comparable in size of the dimensions of the shock tube operating channels used in [1, 2, 5] for their generation. The present studies were performed in shock tubes which insured achievement of equilibrium parameter values behind the incident shock wave front. In addition to performing the experiments, the effect of volume fraction of the c-phase was analyzed, as was the validity of the assumptions of gas idealness and incompressibility of the c-phase normally employed in calculating incident and reflected shock wave parameters.

The studies of shock wave propagation in foams were carried out in a horizontally oriented shock tube with inner diameter of 67 mm. The low-pressure chamber was 5.9 m long, and the high-pressure chamber, 2.6 m. A special laboratory foam generator was used to completely fill the low-pressure chamber. The lateral surface of the shock tube was provided with piezoceramic pressure sensors with a natural resonant frequency of 30 kHz, while the tube face carried a pressure sensor with sensitive element of electretized polyvinylchloride [9] with resonant frequency of 400 kHz, which had a linear dependence of charge generated upon pressure over the range 0.1-100 MPa.

The air pressure in the high-pressure chamber was varied over the range 5-13 MPa. Uncertainty in determining shock wave velocities was no more than 10%, with pressure measurement uncertainty no more than 15%. The mass concentration of liquid in the foam was varied from 2.5 to 27 kg/m^3. The liquid used for the foam was water with 5% of the industrial foam generating agent OP-1 added.

As in [1, 2], two types of incident shock waves were observed – disperse, with a two-front pressure profile configuration at $D_1 < a_0$ (where a_0 is the speed of sound in the gas filling the foam cells), and single-front at $D_1 > a_0$. Increase in liquid concentration while maintaining other conditions equal to leads to a reduction in shock wave velocity and an increase in the pressure head at the front. The velocity and amplitude of the waves studied in the operating section of the low-pressure chamber, where parameters were measured, were constant within the limits of experimental uncertainty over all baselines between recording sensors.

Figure 1 shows a typical recording of shock wave propagation and reflection from a rigid wall in foam with σ_l = 27 kg/m^3, where I, II are the incident and reflected waves, respectively. Also shown are sensor locations along the shock tube. As is evident from the recordings, the pressure profile of the incident shock wave formed has a clearly expressed relaxation zone of two-front configuration. The shock wave velocity in the foam was 320 m/sec, with pressure change at the front of 2.9 MPa. Judging from the oscillograms the length of the relaxation zone $\sim$1.3 m.

Figure 2 shows the experimentally determined dependence of the pressure ratio p_1/p_0, where p_1 is the pressure in the incident wave and p_0 is the initial pressure, upon Mach

Kiev. Translated from Zhurnal Prikladnoi Mekhaniki i Tekhnicheskoi Fiziki, No. 1, pp. 106-114, January-February, 1985. Original article submitted December 26, 1983.

 0021-8944/85/2601-0096$09.50

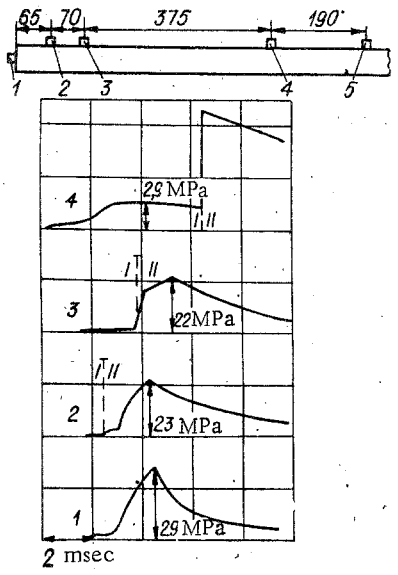

Fig. 1

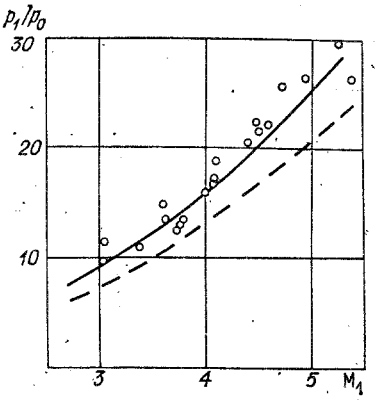

Fig. 2

number $M_1 = D_1/\alpha_0$, where α_0 is the equilibrium speed of sound in the foam.

In contrast to the incident shock waves, the speed and pressure profile of the reflected waves did not remain constant, but varied with removal from the reflecting wall. We will consider the evolution of the reflected wave in the foam, shown in Fig. 1. As is evident from the reflected wave recordings, as it departs from the tube face there is a qualitative change in the pressure profile. Thus, on the tube face the maximum pressure head, achieved in the wave after 2.5 msec comprises $\Delta p_2 = 29$ MPa. The reflection coefficient is then equal to $\Delta p_2/\Delta p_1 = 10$. In contrast to the incident wave the reflected wave has a triangular pressure profile. With increase in pressure a precursor is clearly distinguishable, as in the incident shock wave. At a distance of 65 mm the maximum pressure head in the wave decreases to 23 MPa, and the precursor becomes shorter. The precursor then disappears, there is an abrupt increase in slope of the front, and at a distance of 0.51 m from the face the wave has the steep shock front characteristic of shock waves in gases, with the pressure falloff behind the front becoming smoother and the pressure head at the front decreasing to 12 MPa.

Analysis of the reflected wave velocity measurements reveals that upon departure from the rigid wall over the 0-65-mm base the wave has a velocity $D_2 = 95$ m/sec, while over 65-135 mm the velocity decreases to 55 m/sec, and then begins to increase abruptly, reaching 140 m/sec between sensors 3 and 4, and 470 m/sec between 4 and 5.

Figure 3 generalizes the experimental data on the pressure ratio p_2/p_1 as a function of p_1/p_0 in the reflected waves for gas–liquid foams with various initial densities. The dark circles denote the experimental results of [2]. It is evident that the experimental data obtained herein are higher than the reflection coefficients for air (curve 1), filling the foam cells, and higher than the results of [2].

To analyze the experimental dependences obtained, we will consider the foam as a homogeneous medium consisting of a uniformly distributed liquid phase in a gas. Let a steady-state shock wave propagate within this medium with velocity D_1, and be reflected from a rigid wall at velocity D_2. For the flow region where kinematic equilibrium is established between the phases we will find the interrelationship of medium parameters before and after the fronts of the incident and reflected shock waves. For variables we will use the pressure p, mass velocity u, and temperature T of the gas, the density of the two-phase medium $\rho = \sigma_l + \sigma_g$, the ratio of mass concentrations of liquid σ_l and gas σ_g, $\eta = \sigma_l/\sigma_g = \varepsilon\rho_l/[(1-\varepsilon)\rho_g]$, and the temperature of the c-phase t. Here ε, ρ_l are, respectively, the volume fraction and density of the c-phase, ρ_g is the gas density. The subscript 0 denotes parameters of the unperturbed medium, while 1 and 2 denote values behind the fronts of the incident and reflected waves. Here and below the subscripts g and l indicate parameters of the gas and c-phases, respectively. Assuming that ahead of the incident shock wave front the medium is in equilibrium and at rest ($u_0 = 0$), we write the system of defining equations in the following form:

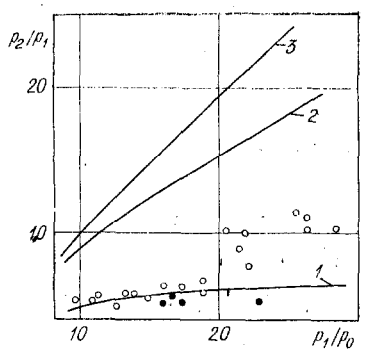

Fig. 3

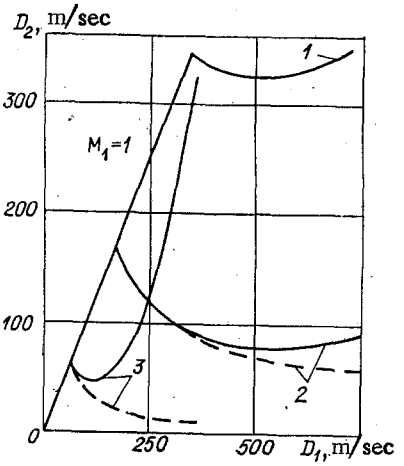

Fig. 4

for the incident shock wave

$$\rho_1(D_1 - u_1) = \rho_0 D_1,\ p_1 - p_0 = \rho_0 D_1 u_1,$$
$$h_1 + (D_1 - u_1)^2/2 = h_0 + D_1^2/2; \tag{1}$$

for the wave reflected from a rigid fixed wall

$$\rho_2 D_2 = \rho_1(D_2 + u_1),\ p_2 - p_1 = \rho_2 D_2 u_1,$$
$$h_1 + (D_2 + u_1)^2/2 = h_2 + D_2^2/2, \tag{2}$$

where h is the specific enthalpy of the mixture, additively determined. For the assumptions normally made, that the gas obeys the equation of state of an ideal gas, and that the c-phase is incompressible and has constant specific heat, the equation of state of the two-phase medium can be written in the form

$$h = \frac{h_g + \eta h_l}{1+\eta} = \frac{1}{1+\eta}\left[\frac{\gamma}{\gamma-1}\frac{p}{\rho_g} + \eta\left(ct + \frac{p}{\rho_l}\right)\right] = \frac{\Gamma - \varepsilon}{\Gamma - 1}\frac{p}{\rho}, \tag{3}$$

where Γ is the effective shock adiabat index, defined by the expression

$$\Gamma = \gamma\frac{1 + \eta\delta\frac{t}{T}}{1 + \gamma\eta\delta\frac{t}{T}}; \tag{4}$$

where $\delta = c/c_p$ is the ratio of the c-phase specific heat to the specific heat of the gas at constant pressure c_p; γ is the gas specific heat ratio.

With the assumptions made above, the interrelationship between the volume content of the c-phase and the densities of the medium and the gas phase is specified by the equation

$$\varepsilon_i/\varepsilon_{i-1} = \rho_i/\rho_{i-1} = (1 - \varepsilon_i)\rho_{gi}/[(1 - \varepsilon_{i-1})\rho_{gi-1}]. \tag{5}$$

If the index Γ in Eq. (3) remains constant both ahead of and behind fronts of the incident and reflected waves, then the interrelationships of medium parameters will be defined by expressions obtained by substituting Eqs. (3)-(5) in Eqs. (1), (2) of the following form:

$$\rho_{gi}/\rho_{gi-1} = [(\Gamma + 1)p_i + (\Gamma - 1)p_{i-1}]/[(\Gamma - 1)p_i + (\Gamma + 1)p_{i-1}]; \tag{6}$$

$$\frac{\rho_{i-1}}{\rho_i} = \frac{\rho_{gi-1}}{\rho_{gi}} + \frac{2\varepsilon_{i-1}(p_i - p_{i-1})}{(\Gamma+1)p_i + (\Gamma-1)p_{i-1}}; \tag{7}$$

$$\frac{T_i}{T_{i-1}} = \frac{p_i}{p_{i-1}}\frac{\rho_{gi-1}}{\rho_{gi}}; \tag{8}$$

$$u_1 = (p_1 - p_0)\sqrt{\frac{2}{\rho_{g0}(1+\eta)[(\Gamma+1)p_1 + (\Gamma-1)p_0]}}; \tag{9}$$

$$D_1 = \frac{1}{1-\varepsilon_0}\sqrt{\frac{(\Gamma+1)p_1 + (\Gamma-1)p_0}{2\rho_{g0}(1+\eta)}}; \tag{10}$$

$$\frac{p_2}{p_1} = \frac{(3\Gamma - 1)\, p_1 - (\Gamma - 1)\, p_0}{(\Gamma - 1)\, p_1 + (\Gamma + 1)\, p_0}; \tag{11}$$

$$D_2 = u_1 \left[\frac{(\Gamma + 1)\, p_2 + (\Gamma - 1)\, p_1}{2(1 - \varepsilon_1)(p_2 - p_1)} - 1 \right]; \tag{12}$$

$$\frac{D_2}{D_1} = \frac{2[p_1(\Gamma - 1) + p_0]}{(\Gamma + 1)\, p_1 + (\Gamma - 1)\, p_0} + \frac{2\varepsilon_0 (p_1 - p_0)[(3\Gamma - 1)\, p_1 + (\Gamma + 1)\, p_0]}{[(\Gamma - 1)\, p_1 + (\Gamma + 1)\, p_0][(\Gamma + 1)\, p_1 + (\Gamma - 1) p_0]}. \tag{13}$$

In particular, the expressions obtained are valid for the two characteristic cases of complete thermal equilibrium and frozen heat exchange between the phases. In fact, in the first case at T = t the adiabatic index Γ coincides with the Poisson adiabatic index for a two-phase mixture Γ_0 which remains constant during passage and reflection of a shock wave. With frozen heat exchange between the phases ($t = t_0$) the index Γ is not constant, but in this case the internal energy of the c-phase remains constant during the shock compression process, which in turn makes it possible to write equation of state (3) in the form

$$h = \frac{p}{\rho} \frac{\Gamma - \varepsilon}{\Gamma - 1} = \frac{p}{\rho} \frac{\gamma - \varepsilon}{\gamma - 1} + \text{const}.$$

Then, as follows from Eqs. (1), (2), Eqs. (6)-(13) become valid for description of the process of shock wave passage and reflection in the case of frozen heat exchange between the phases when in place of Γ we use the Poisson adiabatic index γ, which in contrast to Γ does not change during shock compression of the mixture.

Analysis of Eqs. (6)-(13) permits the conclusion that the density and temperature ratios, the gas temperature, and the pressure and mass velocity of the two-phase medium behind the shock wave are independent of the volume ε occupied by the c-phase, and are completely determined by the degree of heating of the c-phase. At the same time, the density of the medium and the velocity of the reflected wave depend on both the heating and the volume content of the c-phase. We note that for frozen heat exchange between the phases the reflection pressure and gas temperature behind the front coincide with the parameters of a shock wave in a pure gas for given p_1/p_0.

In analysis of shock wave flows in gas suspensions and foams ε is often neglected, assuming that the density of the medium $\rho = \sigma\zeta + \rho_g$. This significantly simplifies calculation of the hydrodynamic problems, introducing an error in determination of the parameters of the incident shock waves no larger than a quantity proportional to $(1 - \varepsilon_0)^{-1}$. A completely different pattern is found when reflected shock waves are considered. Figure 4 shows the effect of ε on reflected shock wave velocity as a function of incident wave velocity. The solid lines are calculated dependences with consideration of ε, the dashed lines, without. Curve 1 was constructed for air, curve 2 for a water–air foam with $\sigma\zeta = 2.5$ kg/m^3, $\varepsilon_0 = 0.0025$, $\Gamma_0 = 1.030$, curve 3, $\sigma\zeta = 27$ kg/m^3, $\varepsilon_0 = 0.027$, $\Gamma_0 = 1.0029$. As is evident from the graphs, neglect of the volume fraction of the c-phase leads not only to quantitative differences, but to a qualitative difference in the dependence of reflected wave velocity on intensity. Thus with nonconsideration of ε the reflected wave velocity decreases with increase in incident wave velocity, but increases when this factor is considered.

For the case of wave propagation in foam presented in Fig. 1 the experimental values of reflected wave velocity near the rigid wall are below the calculated value of 270 m/sec. This fact, like the initial reduction in velocity with subsequent increase with departure of the wave from the rigid wall, can be explained qualitatively by subsequent reflection of portions of the relaxation zone with an increasing concentration of c-phase in the medium. Then the transition from smooth pressure increase to abrupt shock front is in all probability related to exit of the reflected wave onto the foam–gas contact surface.

We will now turn to a comparison of calculated and experimental pressure values in the incident and reflected shock waves. From Eqs. (6)-(10) the dependence of pressure ratio on shock wave Mach number in the foam can be written in the form

$$p_1/p_0 = [2\Gamma M_1^2 - (\Gamma - 1)]/(\Gamma + 1), \tag{14}$$

where $M_1 = D_1/\alpha$ is the shock wave Mach number, α is the speed of sound in the foam, defined by the expression $\alpha = \sqrt{\frac{\Gamma p_0}{[\rho_0 (1 - \varepsilon_0)]}}$.

For the foams studied at thermodynamic equilibrium between the phases $\Gamma = \Gamma_0 \approx 1$ and $p_1/p_0 \approx M_1^2$. This function is shown by the solid line in Fig. 2. The dashed line shows the

dependence obtained by use of the equation $\Gamma = K = 1 + (\gamma - 1)(1 - \varepsilon_0)$, proposed in [4] for description of shock waves in gas–liquid media. For the foams studied K practically coincides with γ. As is obvious, the experimental results for the incident shock waves agree with the calculated parameters with $\Gamma = \Gamma_0$, which indicates attainment of thermodynamic equilibrium between the phases behind the incident wave shock front. At the same time, the parameters of the reflected wave differ significantly from the calculated values. In Fig. 3 curves 2, 3 correspond to calculated equilibrium dependences of p_2/p_1 on p_1/p_0 for foams with $\sigma\zeta$ = 2.5 and 2.7 kg/m^3, respectively. The curve constructed for the case $\Gamma = K$ in fact coincides with the curve 1, constructed for shock wave reflection in a pure gas. Comparison of calculated and experimental values of the reflection coefficients shows that the data obtained differ significantly from equilibrium parameters at $\Gamma = \Gamma_0$, and from the calculated parameters at $\Gamma = K$.

Considering the high shock compressibility of the foam structure, it was assumed that one of the causes of such great divergence between experimental and calculated results may be nonconsideration of the real properties of the foam phase.

To clarify the effects of nonideality of the gas and compressibility of the liquid, shock wave parameters in a foam were calculated using the equations of state of real air and water, obtained by interpolating tabular data on thermodynamic parameters of water and air [10-12]. System (1)-(3) is supplemented by the equations

$$\rho_g^{-1} = \left[\frac{RT}{p + \frac{a}{T(\rho_g^{-1} + d)^2}} + b\right]\left[1 + \frac{\delta_1 p + \delta_2 p(400 - p)}{T - 245}\right]; \tag{15}$$

$$\rho_l^{-1} = 3.086\cdot 10^{-3} - 8.99017\cdot 10^{-4}(374.1 - t)^{0.147166} - \tag{16}$$

$$- 3.9\cdot 10^{-4}(385 - t)^{-1.6}\ (p - 225.5) + a_1 + a_2 t + a_3 t^2 + a_4 t^3 + a_5 t^4 + a_6 p$$

$$+ a_7 p^2 + a_8 p^3 + a_9 p^4 + a_{10} pt + a_{11} pt^2 + a_{12} p^2 t + a_{13} pt^3;$$

$$h_g = b_1 + b_2 T + b_3 T^2 + b_4 T^3 + b_5 T^4 + b_6 p + b_7 p^2 + \tag{17}$$

$$+ b_8 p^3 + b_9 p^4 + b_{10} pT + b_{11} pT^2 + b_{12} p^2 T + b_{13} pT^3;$$

$$h_l = c_1 + c_2 t + c_3 t^2 + c_4 t^3 + c_5 t^4 + c_6 p + c_7 p^2 + c_8 p^3 + c_9 p^4 + c_{10} pt + c_{11} pt^2 + c_{12} p^2 t + c_{13} pt^3, \tag{18}$$

where

$$R = 2.87\cdot 10^{-3};\ a = 0.351273;\ b = 1.0432\cdot 10^{-3};$$

$$\delta_1 = 9.5075\cdot 10^{-4};\ \delta_2 = 9.875\cdot 10^{-6};$$

$$a_1 = 5.7126\cdot 10^{-5};\ a_2 = -8.6109\cdot 10^{-7};\ a_3 = 4.3265\cdot 10^{-9};$$

$$a_4 = -1.6287\cdot 10^{-11};\ a_5 = 2.5868\cdot 10^{-14};\ a_6 = 1.2751\cdot 10^{-8};$$

$$a_7 = -4.9404\cdot 10^{-11};\ a_8 = 1.9303\cdot 10^{-13};\ a_9 = 1.9355\cdot 10^{-16};$$

$$a_{10} = 2.1574\cdot 10^{-10};\ a_{11} = -6.2634\cdot 10^{-13};\ a_{12} = -1.0482\cdot 10^{-13};$$

$$a_{13} = 1.8728\cdot 10^{-15};$$

$$b_1 = -3.5676\cdot 10^5;\ b_2 = 5046.5;\ b_3 = -17.299;$$

$$b_4 = 3.3113\cdot 10^{-2};\ b_5 = -2.3919\cdot 10^{-5};\ b_6 = -1.6957\cdot 10^3;$$

$$b_7 = 0.8302;\ b_8 = -2.0286\cdot 10^{-4};\ b_9 = 2.4283\cdot 10^{-7};$$

$$b_{10} = 9.9132;\ b_{11} = -2.2796\cdot 10^{-2};\ b_{12} = -1.5718\cdot 10^{-3};$$

$$b_{13} = 1.9714\cdot 10^{-5};$$

$$c_1 = 756.18;\ c_2 = 4161.7;\ c_3 = 2.433\cdot 10^{-1};$$

$$c_4 = -6.3329\cdot 10^{-4};\ c_5 = 7.7487\cdot 10^{-6};\ c_6 = 91.087;$$

$$c_7 = 5.6127\cdot 10^{-2};\ c_8 = -1.4895\cdot 10^{-4};$$

$$c_9 = 1.0315\cdot 10^{-7};\ c_{10} = -2.48429\cdot 10^{-1};\ c_{11} = 1.0493\cdot 10^{-5};$$

$$c_{12} = 6.6799\cdot 10^{-5};\ c_{13} = -2.2016\cdot 10^{-7};$$

ρ_g, $\rho\zeta$ are the gas and liquid densities, kg/m^3; h_g and $h\zeta$ are the specific enthalpies, J/kg; pressure, Pa; temperature T, K; t, °C.

The first part of Eq. (16), which does not contain the coefficients a_j, was taken from [10]. The additional term with a_j was added to increase the accuracy of the tabular data approximation. The system of nonlinear equations (1)-(3), (15)-(18) was solved by computer using Newton's method. The relative uncertainty of the solution produced by inaccuracy in

TABLE 1

Component properties	σ_l, kg/m³	D_1, m/sec	$\frac{T_1}{T_0}$	ε_1	$\frac{\rho_1}{\rho_0}$	$\frac{\rho_{g1}}{\rho_{g_0}}$	D_2, m/sec	$\frac{T_2}{T_0}$	ε_2	$\frac{\rho_2}{\rho_0}$	$\frac{\rho_{g2}}{\rho_{g0}}$	$\frac{p_2}{p_1}$	$\frac{\rho_{l2}}{\rho_{l0}}$
$p_1/p_0 = 10$													
Ideal	0	1020	2,62	0	3,81	3,81	459	5,75	0	11,3	11,3	6,50	1
»	2,5	529,3	1,15	0,021	8,56	8,72	79,3	1,30	0,148	59,1	69,1	8,96	1
Real	2,5	529,0	1,15	0,022	8,65	8,82	81,6	1,31	0,152	58,2	68,5	9,08	0,957
Ideal	12,5	274,4	1,03	0,110	8,75	9,70	62,1	1,06	0,538	43,0	91,8	9,75	1
Real	12,5	274,2	1,03	0,111	8,86	9,85	62,5	1,06	0,544	43,3	93,8	9,89	0,999
Ideal	27	192,5	1,01	0,215	7,95	9,86	70,6	1,02	0,728	26,9	96,1	9,88	1
Real	27	192,3	1,01	0,218	8,05	10,0	71,0	1,03	0,733	27,1	99,0	10,0	1,002
$p_1/p_0 = 30$													
Ideal	0	1757	5,97	0	5,03	5,03	631	12,3	0	16,3	16,3	6,69	1
»	2,5	916,4	1,44	0,050	19,8	20,8	105,4	1,90	0,459	183	338	21,4	1
Real	2,5	916,5	1,45	0,054	19,7	20,8	137,3	1,93	0,438	145	257	21,9	0,826
Ideal	12,5	475,3	1,09	0,258	20,6	27,4	182,2	1,19	0,898	71,7	696	27,6	1
Real	12,5	475,2	1,10	0,262	20,7	27,8	191,5	1,21	0,844	69,7	442	28,2	1,035
Ideal	27	333,4	1,04	0,444	16,4	28,8	271,3	1,08	0,957	35,3	796	28,8	1
Real	27	333,3	1,04	0,449	16,6	29,2	264,7	1,09	0,928	36,1	486	28,8	1,054

approximating the thermodynamic parameters of air and water over the pressure range 0.1-90 MPa and temperatures of 293-600°K for calculated shock wave parameters in the range $8 \leqslant p_1/p_0 \leqslant 30$; $2.5 \leqslant \sigma_l \leqslant 27$ kg/m^3 did not exceed 0.5% for D_1, 5.2% for D_2, 1.6% for p_2/p_1. Table 1 presents results of equilibrium shock wave parameter calculations for air and foam with various liquid concentrations.

The significant difference between shock wave parameters in air and foam cells attention to itself. The presence of a c-phase leads to an abrupt increase in compressibility of the medium, significantly exceeding the compressibility of a pure gas. In fact, in intense waves there is a qualitative change in the structure of the medium: the foam behind the reflected wave should most probably be considered a bubble foam, with volume gas content approaching several percent. A comparison of the compressibilities of gas phase in the foam upon shock reflection is still more revealing. Thus, for the case presented in Fig. 1, attainment of equilibrium shock wave reflection should be accompanied by an increase in gas density of 500 times, with $\rho_l/\rho_g = 1.82$. We note that in a gas at $\gamma = 1.4$ the limiting compression in the reflected shock wave comprises $\rho_2/\rho_0 = 21$.

Comparison of the calculation results with and without consideration of real foam phase properties shows that at a pressure in the front of 1-1.5 MPa the uncertainty in determining medium parameters lies within the computational uncertainty introduced by inaccuracy in approximating the equations of state (see Table 1, $p_1/p_0 = 10$). With increase in shock wave intensity ($p_1/p_0 = 30$) the real properties of the gas and c-phases begin to manifest themselves. This reduces the gas density, while the liquid density may be either greater or less than the "ideal" value, depending on temperature. At $p_1/p_0 = \text{const}$ a decrease in liquid concentration increases its temperature. As a consequence, despite the high pressure, expansion of the liquid occurs. The combined effect of decreases in liquid and gas density leads, in particular, to small deviations at relatively low liquid concentrations ρ_2, and thus D_2, from the ideal case (see Table 1, $\sigma_l = 2.5$ kg/m^3). On the other hand, for large liquid concentrations reduction in gas density and compression of the c-phase can not only compensate each other, but lead to a relative increase in density of the two-phase medium. As is evident from Table 1 ($\sigma_l = 27$ kg/m^3) the velocity of the reflected wave becomes less than the "ideal" value.

On the whole, over the range of shock wave intensities and liquid concentrations studied the relative deviation of the shock wave parameters with and without consideration of real properties of the gas and c-phases does not exceed 1% for D_1, 2.5% for D_2, and 3% for p_2/p_1. Thus, within such accuracies analytical expressions (4)-(13) can be used to determine equilibrium shock waves in foams. With reference to incident shock waves this has been confirmed by the experimental studies performed. On the other hand, consideration of the real properties of the medium does not explain the large differences observed between experimental and calculated parameters for reflected waves.

The cause of noncorrespondence between measured and calculated parameter should apparently be sought in the relaxation character of shock wave reflection, caused by sequential reflection of microvolumes of the medium in which the degree of perfection of momentum and energy exchange processes differs.

Exit of the perturbations which then develop onto an "unconnected" contact surface is accompanied by generation of a rarefaction wave in the direction of the reflecting surface. This, in particular, is one of the causes of change of the rectangular profile of the maximum pressure zone in the incident wave into a triangular one in the reflected wave. The effect of these factors on reflected wave parameters can be neglected only if the extent of the equilibrium parameter zone in the wave significantly exceeds the length of the relaxation zone. The maximum dimensions of the thermodynamic equilibrium zones behind the incident and reflected wave fronts may be estimated from Table 1. In particular, for a low-pressure chamber length of 5.9 m for $\sigma_l = 27$ kg/m^3 (see Fig. 1) the length of the equilibrium parameter zone for the incident wave $l_1 = 0.35$ m, while for the reflected wave $l_2 = 0.16$ m. In the observed waves the relaxation zone for both incident and reflected waves is several times greater than the calculated size of the foam samples with equilibrium parameters, so that the zone with thermodynamically equilibrium parameters is not reflected directly from the rigid wall, but through a layer of nonequilibrium two-phase medium, included in the relaxation zone. In this case use of Eqs. (4)-(13) is not justifiable, and despite the steady-state and equilibrium character of the incident shock waves, the reflection coefficients will be lower than calculated values. At the same time, since increase in length of the shock tube operating section leads to a relative increase in the equilibrium parameter zone, this should lead to

an increase in reflection pressure, as was confirmed in experiment. The above indicates the validity of the proposed physical analysis of the results obtained, and indicates the necessity of considering the effects of length of the wave perturbation and pressure profile in the relaxation zone zone on reflected wave parameters in two-phase media.

For a deeper understanding of the observed phenomena it will be necessary to analyze the effect of relaxation processes on formation and reflection of shock waves in foam.

LITERATURE CITED

1. V. M. Kudinov, B. I. Palamarchuk, et al., "Shock waves in gas–liquid media with foam structure," Prikl. Mekh., 13, No. 3 (1977).
2. A. A. Borisov, B. E. Gelfand, et al., "Shock waves in water foams," Acta Astronaut., 5, 1027 (1978).
3. B. E. Gel'fand, A. V. Gubanov, and E. I. Timofeev, "Peculiarities of shock wave propagation in foams," Fiz. Goreniya Vzryva, No. 4 (1981).
4. E. I. Timofeev, B. E. Gel'fand, et al., "Effect of the volume fraction of gas on shock wave characteristics in gas–liquid media," Dokl. Akad. Nauk SSSR, 268, No. 1 (1983).
5. J. S. Krasinski, A. Khosla, and V. Ramech, "Dispersion of shock waves in liquid foams of high dryness fraction," Arch. Mech. Stosow., 30, Nos. 4-5 (1978).
6. L. I. Sedov, Similarity and Dimensionality Methods in Mechanics [in Russian], Nauka, Moscow (1972).
7. B. I. Palamarchuk, V. A. Vakhnenko, et al., "Effect of relaxation processes on shock wave attenuation in water foams," in: Reports to the IV International Symposium on Use of Explosion Energy [in Russian], Gotvaldov, Czechoslovakia (1979).
8. V. M. Kudinov, B. I. Palamarchuk, et al., "Shock wave parameters in explosions in foam," Dokl. Akad. Nauk SSSR, 228, No. 3 (1976).
9. A. V. Cherkashin, "Piezoeffect in electretized vinyplast under dynamic loading," Fiz. Goreniya Vzryva, No. 3 (1981).
10. M. P. Vukalovich, Thermodynamic Properties of Water and Water Vapor [in Russian], Mashgiz, Moscow (1950).
11. M. P. Vukalovich, S. L. Rivkin, and A. A. Aleksandrov, Tables of Thermodynamic Properties of Water and Water Vapor [in Russian], Standartov, Moscow (1969).
12. A. A. Vasserman, Ya. Z. Kazavchinskii, and V. A. Rabinovich, Thermophysical Properties of Air and Its Components [in Russian], Nauka, Moscow (1966).

INFLUENCE OF SCREENING GAS-SUSPENSION LAYERS ON SHOCK-WAVE REFLECTION

A. I. Ivandaev and A. G. Kutushev

UDC 532.529:518.5

More and more attention has recently been spent on investigating the urgent problem of nonstationary wave flows of gas-suspensions. The main results obtained are reflected in a number of papers [1-4] and are examined in sufficient detail [5]. An analysis of weak shock propagation in gas suspensions is represented in [6] on the basis of the Burgers equation, while strong shocks in a gas with disperse particles are investigated in [7, 8]. Analysis of the literature shows that stationary shock-wave propagation and interaction with obstacles in gas-suspensions have been studied well enough. At the same time there are practically no papers devoted to the investigation of the nonstationary process of finite-duration shocks interacting with obstacles [5].

Results of a numerical investigation of the influence of the screening gas-suspension layer on the reflection of a plane nonstationary shock from a rigid wall are represented in this paper. The results can be useful in the design of systems of dust protection from the action of shocks and the analysis of possibilities of gasdynamics methods of depositing powder coatings [9].

Moscow. Translated from Zhurnal Prikladnoi Mekhaniki i Tekhnicheskoi Fiziki, No. 1, pp. 115-120, January-February, 1985. Original article submitted November 20, 1983.